Title

Hafnium Sulfate Prenucleation Clusters and the Hf18 Polyoxometalate Red Herring

Journal

Inorganic Chemistry, 53(8)

ISSN

0020-1669

Authors

Ruther, Rose E
Baker, Brenna M
Son, Jung-Ho
et al.

Publication Date

2014-04-21

DOI

10.1021/ic500375v

Peer reviewed

Inorganic Chemistry

Article

pubs.acs.org/IC

Hafnium Sulfate Prenucleation Clusters and the Hf_{18} Polyoxometalate Red Herring

Rose E. Ruther,[†,‡] Brenna M. Baker,[†,‡] Jung-Ho Son,[†,§] William H. Casey,[†,§] and May Nyman*[,†,‡]

[†]Center for Sustainable Materials Chemistry and [‡]Department of Chemistry, Oregon State University, Corvallis, Oregon 97331-4003, United States

[§]Department of Chemistry, University of California, Davis, California 95616, United States

Supporting Information

ABSTRACT: In prior studies, aqueous Hf sulfate−peroxide solutions were spin-coated, dehydrated, patterned by electron-beam lithography, ion-exchanged (OH^- for SO_4^{2-}), and finally converted to HfO_2 hard masks via annealing. The atomic-level details of the underlying aqueous chemistries of these processes are complex and yet to be understood. Yet a thorough understanding of this specific chemical system will inspire development of design rules for other aqueous-precursor-to-solid-state metal oxide systems. Often-observed crystallization of the Hf_{18} polyoxometalate from aqueous Hf sulfate−peroxide precursor solutions has led us to believe that Hf_{18} may represent an important intermediate step in this process. However, via detailed solution studies described here (small-angle X-ray scattering, electrospray ionization mass spectrometry, and Raman spectroscopy), we ascertained that Hf_{18} is in fact not a prenucleation cluster of Hf sulfate coatings. Rather, the Hf tetramers, pentamers, and hexamers that are the core building blocks of Hf_{18} are robustly persistent over variable compositions and aging time of precursor solutions, and therefore they are likely the rudimentary building blocks of the deposited thin-film materials. These Hf clusters are capped and linked by sulfate and peroxide anions in solution, which probably prevents crystallization of Hf_{18} during the rapid dehydration process of spin-coating. In fact, crystallization of Hf_{18} from the amorphous gel coating would be detrimental to formation of a high-density conformal coating that we obtain from precursor solutions. Therefore, this study revealed that the well-known Hf_{18} polyoxometalate is not likely to be an important intermediate in the thin-film process. However, its subunits are, confirming the universal importance of deriving information from the solid state, albeit judiciously and critically, to understand the solution state.

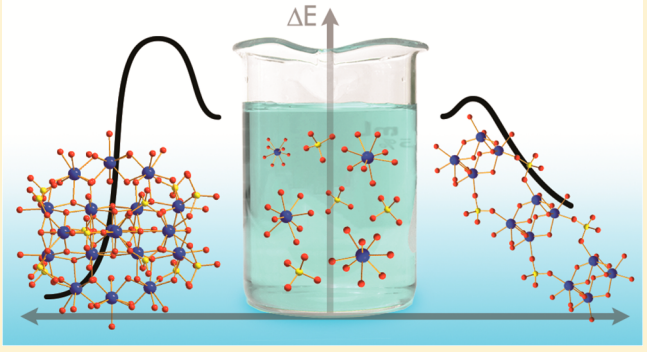

INTRODUCTION

The transition from solution species to solid amorphous or crystalline phases is never straightforward. In particular, aqueous systems are complex when the solvent also serves to link metal cations through processes mediated by pH, concentration, and perhaps noninnocent counterions. Crystallization may be preceded by the formation of an amorphous precursor.[1,2] In the nonclassical theory, nucleation and growth may not occur through the addition of single atoms or molecules but rather through the aggregation of prenucleation clusters or nanoparticles.[3−6] Our interest in understanding and controlling solution speciation stems in part from our desire to deposit high-quality oxide thin films from aqueous solutions.[7,8] By understanding the solution behavior that yields dense, smooth films, we aim to develop design rules that will guide the synthesis of new materials. The sulfates of hafnium and zirconium provide an especially rich and varied class of compounds for understanding the relationship between solution species and solid phases. As Clearfield noted fifty years ago, zirconium sulfate solutions do not contain a single, preferred species that is stable over a range of conditions, and a very large number of both neutral and basic salts of zirconium and hafnium form from solution.[9−12] From a survey of the Inorganic Crystal Structure Data Base (ICSD), the number of structurally characterized zirconium sulfate phases far exceeds the number of hafnium sulfate phases, despite their periodic relationship and thus their presumed chemical similarity. Thus this chemistry warrants focus, starting from the precursor solutions.

Early results from wide-angle X-ray scattering conclude that a tetrameric species $[M_4(OH)_8(H_2O)_{16}]^{8+}$ (M = metal) dominates in solutions of the zirconium and hafnium oxyhalides, consistent with the solid-state structure.[13,14] Small-angle X-ray scattering (SAXS) studies on solutions of $ZrOCl_2$ indicate that the tetramer exists in equilibrium with an octamer, but with high concentrations of added acid ([HCl] ≥ 0.6 M), the tetramer is favored.[15,16] Recent work by Soderholm using high-

Received: February 15, 2014
Published: April 2, 2014

   dx.doi.org/10.1021/ic500375v | Inorg. Chem. 2014, 53, 4234−4242

energy X-ray scattering (HEXS) suggests that even under strongly acidic conditions (4 *m* $HClO_4$), higher-order oligomers form in equilibrium with the tetramer and may include pentameric, hexameric, and/or octameric species.[17] However, one cannot rule out the effect of the perchlorate counteranion. Hexanuclear zirconium[18,19] and hafnium[20,21] clusters with several unique geometries have been characterized by X-ray diffraction including octahedra, capped pentagons, and ring structures that adopt a chair conformation. However, all but one of these possess surface-passivating ligands like glycine. SAXS data indicate the octamer is a prevalent aqueous species, but this is subject to interpretation. Finally, an unusual anionic nonanuclear hafnium sulfate cluster crystallized with ammonium cations was recently characterized.[22] The variety of structures points to the important role pH and counterions play in directing the assembly of hafnium and zirconium clusters from solutions.

Sulfate and peroxide form complexes with zirconium and hafnium,[23−25] and both peroxide[26−30] and sulfate[7,31−37] are commonly used to control the synthesis and properties of Group IVA materials such as nanoparticles, thin films, and mesostructures. Despite widespread use in materials synthesis, few studies have investigated the effect of peroxide ligands on solution speciation, and typically only the solid-state phases are characterized. Notably, very few peroxo complexes of hafnium or zirconium have been isolated.[38−41] This is because, like many metal cations, Zr/Hf^{4+} can catalyze decomposition of peroxide, and the chemistry is hard to control. Zirconium sulfate solutions have been studied by dynamic light scattering,[42] ultracentrifugation,[42] SAXS,[43−46] extended X-ray absorption fine structure,[45−49] and HEXS.[17] Despite differences in solution composition, several investigations conclude that large polynuclear clusters form in these solutions and serve as the building blocks for polymer chains, gel networks, and crystalline precipitates.[43−45,47,48] A zirconium octadecamer, Zr_{18}, first identified by Clearfield in the crystalline phase as $Zr_{18}O_4(OH)_{38.8}(SO_4)_{12.6}{\cdot}33H_2O$, is commonly proposed to be an important species in these solutions.[11] While we are aware of no comparable studies of hafnium sulfate solutions, the isomorphous hafnium octadecamer Hf_{18} has also been characterized in the solid state.[50] Figure 1 shows the structure of the Hf_{18} cluster, along with the hexamer, pentamer, and tetramer building blocks that are pertinent to the later discussion regarding solution speciation. The Hf_{18} cluster is centered by a Hf hexamer, which shares opposite edges with two Hf pentamers, comprising twelve of the Hf polyhedra. Six additional edge-sharing Hf polyhedra, three on each side, bridge the pentamers of the elongate pentamer−hexamer−pentamer unit. The thirteen sulfate anions cap the outside of the structure, and the cluster is neutral. A related structure, Hf_{17}, with a charge of +1, has also been identified; with one Hf tetramer and one Hf pentamer flanking the central hexamer (instead of two pentamers).[51]

Previously, it was shown that highly uniform, dense thin films can be deposited from hafnium sulfate solutions using simple spin-coating techniques.[7] The addition of radiation-sensitive peroxide ligands yields materials that can be directly patterned with UV light or electron beams at very high resolution, and the unpatterned portion plus sulfate ligands are subsequently removed by dissolution in tetramethylammonium hydroxide, leaving behind only hafnium oxyhydroxide, which is thermally annealed.[52−55] While the hafnium sulfate thin films are X-ray amorphous up to 700 °C, Hf_{18} readily crystallizes from the

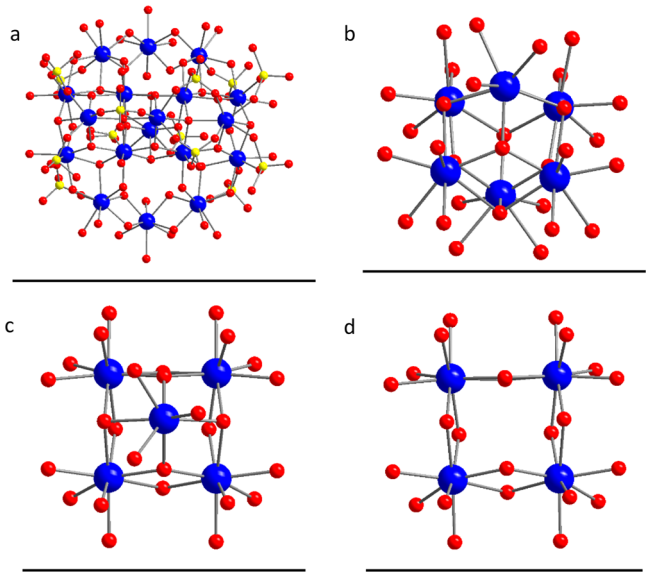

Figure 1. (a) Structure of the Hf_{18} cluster from reference[50] and its core building blocks observed by mass spectrometry (see text). (b) Hf oxo hexamer. (c) Hf oxo pentamer. (d) Hf oxo tetramer. Blue spheres are Hf, yellow spheres are S, and red spheres are O.

precursor solution, with or without peroxide ligands. In this Contribution, SAXS, Raman spectroscopy, and electrospray-ionization mass spectrometry (ESI-MS) are used to characterize aqueous hafnium solutions, the effect of sulfate and peroxide ligands on the formation of polynuclear hafnium clusters, and their assembly into higher-order oligomers. Our findings, somewhat surprising in the disconnect between the solution and the crystalline states, offer a cautionary tale in correlating solid-state structures with solution species and highlight the importance of SAXS and other in situ methods for monitoring cluster formation at critical length scales below 10 nm. In particular, the Hf_{18} cluster can be described as a thermodynamically stable assembly as it crystallizes slowly, whereas thin-film assemblies are obtained by rapid evaporation of water and can be considered metastable. These findings also have significant implications for understanding the formation and lithographic patterning of films formed from metal-oxide clusters.

RESULTS AND DISCUSSION

Raman Spectroscopy. The coordination of sulfate and peroxide ligands to hafnium was studied using Raman spectroscopy. Figure 2 shows the Raman spectra of Hf_{18} powder, a hafnium sulfate solution, and a peroxo hafnium sulfate solution. $HfOCl_2$ (aq), H_2SO_4 (aq), and H_2O_2 (aq) are also shown for comparison. The ν(O−O) vibration in free (uncoordinated) peroxide appears at 876 cm^{-1}, as seen in the spectrum of aqueous hydrogen peroxide. The coordination of peroxide to the hafnium clusters results in a new stretch at 834 cm^{-1} consistent with what has been observed previously for peroxo complexes of hafnium and zirconium.[56−58] The coordination of sulfate to the hafnium clusters can also be followed in the Raman spectra. The ν_1(S−O) symmetric stretch of free (uncoordinated) sulfate and bisulfate appear at 980 and 1050 cm^{-1}, respectively, as seen in the spectrum of pure sulfuric acid.[59] Free sulfate and bisulfate are also present in both the hafnium sulfate and peroxo hafnium sulfate solutions. Coordination to a metal shifts the free sulfate peak toward higher frequencies,[60] and new vibrational modes appear most

dx.doi.org/10.1021/ic500375v | Inorg. Chem. 2014, 53, 4234−4242

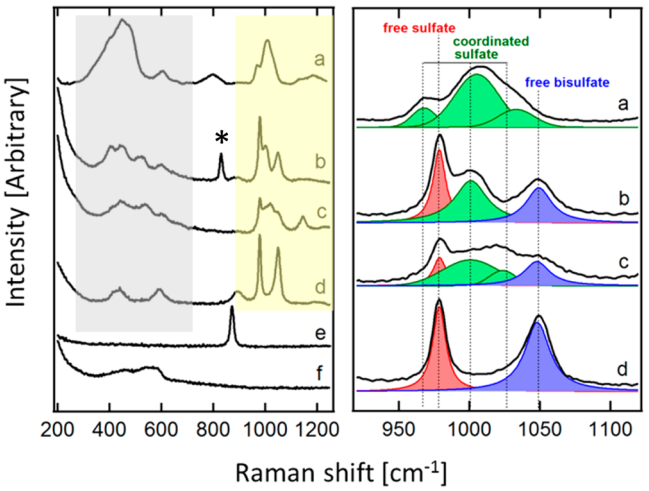

Figure 2. (left) Raman spectra of solid Hf_{18} (a), 200 mM hafnium sulfate solution with peroxide (b), 200 mM hafnium sulfate solution without peroxide (c), 140 mM sulfuric acid (d), 100 mM hydrogen peroxide (e), and 200 mM hafnium oxychloride solution (f). The gray shaded area indicates Hf–O vibrations; the yellow shaded area indicates S–O stretches. The (*) indicates peroxide coordinated to Hf. (right) Enlarged view of the ν_1(S–O) symmetric stretching region for the same solutions.

prominently near 1000 cm^{-1}. The Raman spectrum of Hf_{18} powder consists of three broad, overlapping components in the ν_1, region with peaks at 968, 1006, and 1035 cm^{-1}. The Hf_{18} cluster has nine crystallographically unique sulfate groups, which exhibit three different coordination modes: bidentate/mononuclear, bidentate/binuclear, and tridentate/trinuclear. The S–O bonds range in length from 1.29 to 1.66 Å, which accounts for the broad distribution of vibrational energies.[50]

The hafnium sulfate solutions exhibit vibrational modes similar to those of Hf_{18}, which are characteristic of bidentate (and possibly tridentate) coordination.[17,61−65] Similar spectra have been reported for other metal sulfates in both solution[17,62,63,65,66] and the solid state.[61,67−69] In addition to the stretches due to free sulfate and bisulfate, hafnium sulfate solutions with peroxide have vibrational modes centered at 967 and 1000 cm^{-1}. Hafnium sulfate solutions without peroxide exhibit only one additional very broad peak centered near 1006 cm^{-1}. Blue shifts in the vibrational frequency of the ν_1 mode have been attributed to increasing denticity of sulfate in metal-sulfate solutions.[62−65] In general ν_1(free SO_4^{2-}) < ν_1(monodentate) < ν_1(bidentate). This suggests that sulfate is more highly coordinated in solutions without peroxide. This is consistent with the MS data described later. Significantly more free (uncoordinated) sulfate is measured in solutions with peroxide, which provides further evidence that peroxide competes with sulfate for coordination sites. Large shifts in the ν_1(S–O) mode between 1005 and 1010 cm^{-1} have been attributed to the formation of complex ion aggregates such as chain-like structures found in gels.[62−65] The Hf–O vibrations (along with S–O) are apparent in the low-frequency region of the spectrum, between 400 and 600 cm^{-1}. The solution Raman spectra suggest that sulfate coordination favors the formation of extended structures and that these networks are disrupted by peroxide. Further evidence for this interpretation comes from SAXS analysis discussed below.

SAXS of $HfOCl_2$ Solutions. $HfOCl_2$ solutions were studied at concentrations ranging from 5 mM to 500 mM. Evaluation of the more concentrated solutions (≥50 mM) is complicated by the pronounced structure factor (Coulomb peak) caused by interaction between scatterers. The hafnium tetramer $[Hf_4(OH)_8(H_2O)_{16}]^{8+}$ has a large positive charge,[15] and relatively long-range ordering may occur through the chloride counterions.[70] Different models were therefore used to analyze the low-concentration and high-concentration data. Table 1 presents the radii of gyration (R_g) determined from Guinier and pair distance distribution function (PDDF) analyses of the more dilute solutions. The R_g of clusters in the 5 and 20 mM solutions is between 5 and 6 Å, which is too large to represent only the tetramer even if chloride ions are included in the second coordination shell.[16] Pentamers and hexamers that would form by capping the tetramer have R_g values that are practically indistinguishable from the tetramer. To explain the relatively large value of R_g, prior SAXS studies on $ZrOCl_2$ solutions propose that an octamer forms in equilibrium with the tetramer.[16] The octamer could form by stacking two tetramers on top of each other or by arranging the two tetramers side by side in a single layer. For the earlier zirconium work, slightly better fits to the SAXS intensity data are obtained for the stacked octamer model compared to the sheet octamer model. Our experimental results on dilute $HfOCl_2$ solutions, however, support the formation of the sheet octamer. Figure 3

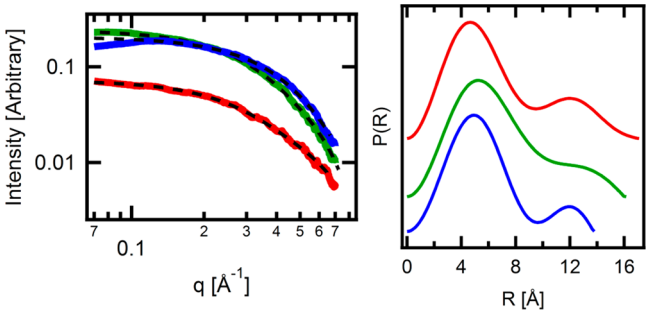

Figure 3. (left) SAXS intensity data for 5 mM (red), 20 mM (green), and 50 mM (blue) $HfOCl_2$ solutions. Dashed lines are fits to a model of monodisperse cylindrical particles. (right) PDDF for the same solutions.

shows the SAXS intensity data for the 5, 20, and 50 mM solutions. The data could not be adequately modeled by assuming simple spherical particles. Rather, an asymmetrical shape is required. Fits to a cylindrical model are shown in Figure 3, and the fit parameters are presented in Table 1. The radius and length of the cylinder are in good agreement with

Table 1. Form Factor Parameters for Dilute $HfOCl_2$ Solutions

$HfOCl_2$ concentration (mM)	R_g from Guinier fit (Å)	R_g from PDDF (Å)	maximum linear extent from PDDF (Å)	χ^2 (PDDF)	radius from cylindrical fit (Å)	length from cylindrical fit (Å)
5	5.9	5.4	17	0.52	2.9	17
20	5.8	5.3	17	0.58	3.8	16
50	4.5	4.5	14	0.71	3.4	12

dx.doi.org/10.1021/ic500375v | Inorg. Chem. 2014, 53, 4234−4242

the sheet octamer model. Further evidence for the octamer layer comes from PDDF analysis, also shown in Figure 3. The shape of the PDDF curve is characteristic of particles with one long and one short axis.[71] The linear extent of the PDDF is also consistent with the long axis of the octamer sheet. As the concentration of the solution increases, the average particle size decreases. The equilibrium shifts toward smaller clusters due to the increasing acidity. While the SAXS data cannot distinguish between tetramers, pentamers, and hexamers, HEXS of similar zirconium solutions suggest that some pentamers and/or hexamers may be present in equilibrium with the tetramer.[17]

Figure 4 presents SAXS intensity data for the higher concentrations of $HfOCl_2$ solutions, both with and without

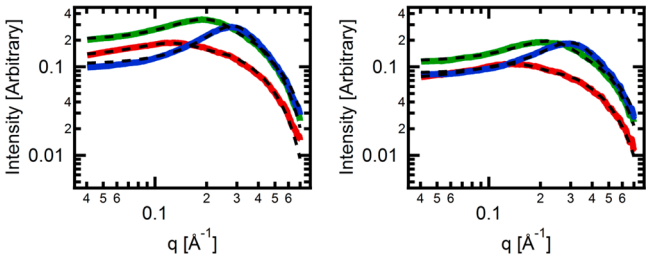

Figure 4. SAXS intensity data for 50 mM (red trace), 200 mM (green trace), and 500 mM (blue trace) $HfOCl_2$ solutions without (left) and with peroxide (right). Dashed lines are fits to a model that assumes monodisperse spherical particles and includes a structure factor due to interparticle interactions.

the addition of hydrogen peroxide. Table 2 summarizes the values of R_g obtained from both the Guinier fits and PDDF analysis. The results are in good agreement with previous SAXS results from $ZrO(NO_3)_2$ and $ZrOCl_2$ solutions.[15,16] At the higher concentrations the equilibrium has shifted away from the octamer, and the data can be fit reasonably well by assuming a simple spherical model for the particle form factor. To account for the Coulomb peak, the interference structure factor[72] was used within the Modeling II macros in IRENA.[73] The spherical radius, η, and φ parameters derived from this model are shown in Table 2. The parameter η corresponds to the average distance between clusters, and φ represents the average number of clusters in the nearest neighbor sphere. As the concentration increases, the average distance between clusters decreases, and the number of nearest neighbors increases.

Notably, R_g and the spherical radius are consistently smaller in the presence of hydrogen peroxide. The R_g of 3.5−4 Å for solutions with peroxide is consistent with the size expected for tetrameric hafnium. The larger size of 4.5−4.6 Å measured in the absence of peroxide suggests that higher-order oligomers, such as hexamers and/or octamers proposed for zirconium solutions, have also formed in equilibrium with the tetramer.[16,17] Two peroxide groups are able to bind to each hafnium tetramer and replace four bridging hydroxyl groups.[25] Peroxide, therefore, acts as a capping ligand that stabilizes the smaller clusters at the expense of larger species.

SAXS of Hafnium Sulfate Solutions. Figure SI1 of the Supporting Information shows SAXS data for different concentrations of hafnium sulfate solutions both with and without peroxide. The Coulomb peak present in the absence of sulfate has disappeared. This can be attributed to the change in charge on the cluster and/or the increase in ionic strength of the solution.[70] Capping clusters with sulfate ligand (as observed in Hf_{18}) neutralizes some positive charge, bringing cluster charge closer to neutral and thus diminishes the ordering mechanism through counterions.

For all concentrations, the average particle size increases significantly with solution aging as indicated by the large increase in intensity for small values of q. The slope in the log−log plots also approaches −1 as the solutions age. This suggests that the larger particles that form are rod-shaped.[74,75] Table 3 summarizes the radii of gyration (R_g) obtained from both the Guinier fits and PDDF analysis for the hafnium sulfate solutions. Also included are fits to a cylindrical model. The length of the cylinder is in good agreement with the maximum linear extent from the PDDF analysis. The cross-sectional radius of 3 to 4 Å is similar in size to a tetrameric building block. Figure 5 shows SAXS intensity data with cylindrical fits for solutions that have aged but not yet formed any visible precipitate.

Further evidence for the formation of linear structures comes from the PDDF analysis. Figure 6 shows the distance distribution function for 500 mM solutions. Initially only small clusters with approximately spherical symmetry are present, consistent with Hf tetramers or hexamers. After 24 h, the linear extent has increased significantly. The shape of the PDDF is characteristic of particles that are cylindrical in shape with periodical changes in electron density along the cylinder axis[71] and suggests that the monomers oligomerize to form chains.[76] Similar PDDFs are obtained for the more dilute solutions, indicating that chain formation is also occurring at the lower concentrations (see Supporting Information, Figure SI2).

The extent of oligomerization depends on the age and concentration of the solution, as well as the presence of peroxide. For the highest concentration studied (500 mM) the

Table 2. Form and Structure Factor Parameters for Higher Concentration $HfOCl_2$ Solutions, with and without Peroxide

solution composition	R_g from Guinier fit (Å)	R_g from PDDF (Å)	maximum linear extent from PDDF (Å)	χ^2 (PDDF)	spherical radius from modeling II (Å)	η (distance between clusters, Å)	φ (number of clusters in nearest neighbor sphere)
50 mM $HfOCl_2$	4.5	4.5	14	0.7	4.9	42	0.5
50 mM $HfOCl_2$ 25 mM H_2O_2	4.1	3.6	10	1.5	4.5	38	0.5
200 mM $HfOCl_2$	N/A[a]	4.5	16	2.5	4.9	27	0.9
200 mM $HfOCl_2$ 100 mM H_2O_2	N/A[a]	3.5	10	2.3	4.4	23	0.9
500 mM $HfOCl_2$	N/A[a]	4.6	13	3.9	4.5	19	2.2
500 mM $HfOCl_2$ 250 mM H_2O_2	N/A[a]	3.6	10	2.5	4.2	17	1.7

[a]Could not be determined due to interferences from structure factor peak.

dx.doi.org/10.1021/ic500375v | Inorg. Chem. 2014, 53, 4234−4242

Table 3. Form Factor Parameters for Hafnium Sulfate Solutions with and without Peroxide

Hf concentration (mM)	age (h)	R_g from Guinier fit (Å)	R_g from PDDF (Å)	maximum linear extent from PDDF (Å)	χ^2 (PDDF)	radius from cylindrical fit (Å)	length from cylindrical fit (Å)
without peroxide (ratio Hf/SO_4 = 1:0.7)							
50	0	7.0	6.9	22	1.84	3.7	22
50	24	8.8	8.7	28	1.52	3.9	29
200	0	7.2	7.4	30	2.28	3.5	21
200	24	12.4	11.8	35	2.95	4.0	47
500	0	3.9	3.6	10	4.10	3.6	8.6
500	24	12.2	12.2	40	1.62	3.9	42
500	72	13.2	14.6	50	0.92	4.0	51
with peroxide (ratio $Hf/SO_4/O_2^{2-}$ = 1:0.7:0.5)							
50	0	3.8	3.8	13	0.78	3.0	11
50	24	3.8	3.9	13	0.54	3.1	11
50	72	4.4	4.5	14	0.53	3.0	13
50	165	6.8	6.9	22	0.36	3.4	21
200	0	3.5	3.5	13	2.26	3.2	9.4
200	24	4.1	4.2	14	0.69	3.0	11
200	72	10.1	10.5	38	1.13	3.7	33
500	0	3.0	3.1	9	7.09	3.5	6.2
500	24	10.0	9.6	37	1.35	3.3	26
500	72	12.8	12.9	40	1.16	3.9	44
500	165	14.2	13.1	40	1.60	4.0	47

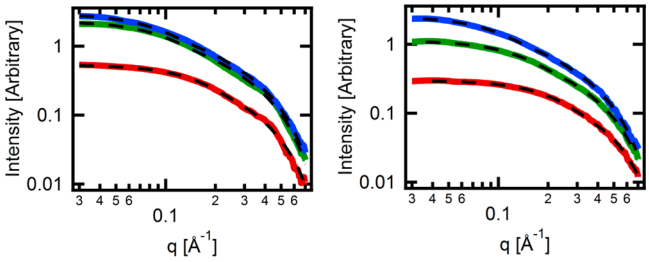

Figure 5. (left) Cylindrical fits (dashed lines) to SAXS intensity data for aged (Hf oxychloride plus sulfate) solutions without peroxide: 500 mM solution aged 72 h (blue), 200 mM solution aged 24 h (green), and 50 mM solution aged 24 h (red). (right) Cylindrical fits (dashed lines) to SAXS intensity data for aged (Hf oxychloride plus sulfate) solutions with peroxide: 500 mM solution aged 7 d (blue), 200 mM solution aged 72 h (green), and 50 mM solution aged 7 d (red).

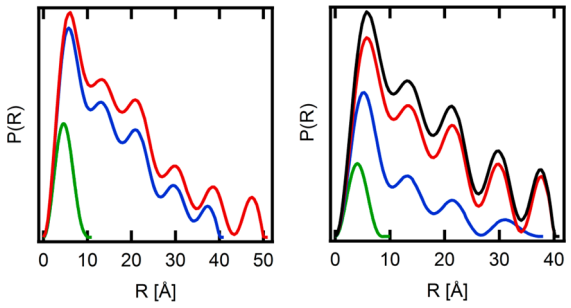

Figure 6. PDDF for 500 mM hafnium sulfate solutions without peroxide (left) and with peroxide (right). Solutions were aged for 0 h (green), 24 h (blue), 72 h (red), and 7 d (black).

initial particle size is smaller than it is at lower concentrations. This is attributed to the increased acidity of these solutions. Solutions without peroxide tend to oligomerize more rapidly than solutions with peroxide. Peroxide is a bidentate, chelating ligand that may hinder hydrolysis condensation similar to ligands more commonly used in sol–gel chemistry such as acetylacetonates or carboxylates.[30] The addition of hydrogen peroxide to the precursor solution delays the onset of precipitation for days or weeks, but slow peroxide decomposition ultimately yields the same Hf_{18} crystalline precipitate. Characterization by single-crystal X-ray diffraction indicates that no peroxide groups are present in the solid, in agreement with prior structural studies.[50] The largest R_g measured prior to precipitation is approximately 1.5 nm, and the largest linear extent is 5 nm.

Since the Hf_{18} precipitates from these solutions, an obvious question is whether the same cluster is a significant species in solution, as has been proposed for the analogous zirconium sulfate solutions.[17,43−45,47,48] The Hf_{18} forms chains in its crystalline lattice, and short oligomers could be present in solution and act as building blocks for the crystalline product. The maximum linear extent measured for the hafnium sulfate solutions is around 5 nm, which corresponds to a chain of three Hf_{18} clusters. Therefore, scattering data was simulated for the single cluster, a dimer, and a chain of three clusters using solX software.[77,78] The simulated SAXS intensity curves as well as PDDF analysis are shown in Figure 7. The Hf_{18} cluster has an irregular shape with variable diameter ranging from 12 to 17 Å for different axes through the center. This low symmetry leads

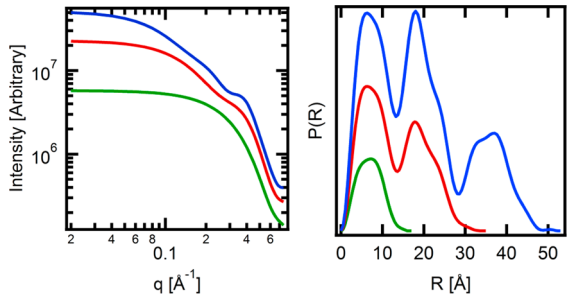

Figure 7. (left) SAXS intensity data simulated using solX for Hf_{18} chains with one (green), two (red), and three (blue) clusters. (right) PDDF for Hf_{18} chains derived from the intensity data above using macros in IRENA.[73]

dx.doi.org/10.1021/ic500375v | Inorg. Chem. 2014, 53, 4234−4242

to very characteristic features in the PDDF. Specifically, each cluster contributes two closely overlapping peaks to the PDDF. The PDDF analysis of the experimental data does not exhibit this pattern. Rather, the experimental PDDF data show regularly spaced peaks, which generally decrease in intensity monotonically. This suggests that the monomer building block for the observed chains is smaller than the Hf_{18} cluster. Further evidence that the Hf_{18} is not a major component in solution comes from the cylindrical fits to the experimental and simulated data. The chain of three Hf_{18} clusters was fit to a cylindrical model with length = 52.7 Å and cross-sectional radius = 5.40 Å. These values are in excellent agreement with the actual dimensions derived from the crystal structure. The cross-sectional radii determined from the experimental data range from approximately 3 to 4 Å, which are too small to be derived from Hf_{18}.

While SAXS data are obviously insufficient to propose a detailed molecular model for the oligomers, it is nonetheless instructive to compare these results to other solution studies as well as solid-state structures. Both EXAFS[49] and HEXS[17] analyses of zirconium sulfate solutions show correlations at approximately 3.6 and 5.0 Å, which are attributed to hydroxy-bridged Zr and diagonal Zr−Zr correlations in the tetrameric unit. It therefore seems likely that at least some of the tetrameric units are preserved in the hafnium sulfate solutions, especially at the early stages of cluster growth. The cross-sectional radius of 3 to 4 Å is consistent with a tetrameric unit, and fragments of the Hf_{18} cluster are structurally very similar to the tetramer. Since linear structures are forming in solution, the basic sulfates that form chains in the solid state are also of interest. Basic hafnium and zirconium sulfates of the series $M(OH)_2SO_4{\cdot}nH_2O$ (n = 0, 1, 3) consist of infinite chains of $[M(OH)_2]_n^{2n+}$ bridged by sulfate groups.[79−83] The "equator" of the Hf_{18} cluster consists of a similar framework with a ring of 10 edge-sharing Hf ions linked by double oxo or hydroxo bridges. Enclosed within this chain is the more highly polymerized core. The Hf_{18} is unique in that it reflects structural motifs from both zero- and one-dimensional crystals. Similarly, SAXS studies of the hafnium sulfate solutions reveal both the zero-dimensional clusters present at early stages followed by the formation of one-dimensional chains as the solutions age.

These results indicate that the relationship between the species in hafnium sulfate solutions and the crystalline precipitate is indirect. The Hf_{18} is a neutral cluster, and the related Hf_{17} cluster has only a +1 charge, which leads to very low solubility in water. Our efforts to redissolve the Hf_{18} precipitate in dilute HNO_3 (aq) or HCl (aq) and isolate single clusters yielded only larger species or smaller fragments (see Supporting Information, Figure SI3). The mother liquor that remained postprecipitation was also analyzed. After three weeks at room temperature, Hf_{18} formed in 80% yield from a 500 mM solution. Hafnium clusters with R_g = 4.3 Å remained in solution. The small size suggests that the mother liquor consists primarily of highly soluble tetrameric species with a small number of larger clusters such as pentamers, hexamers, and/or octamers. Further evidence for this interpretation comes from the PDDF analysis, which is in agreement with mostly the tetramer and/or hexamer, and a small concentration of the side-by-side octamer (see Figure 7 and Supporting Information, Figure SI4). There is no evidence for clusters as large as the Hf_{18} or long chain-like oligomers in the mother liquor. These results are consistent with the low solubility of Hf_{18}, which precipitates as soon as it forms. The high yield of Hf_{18} from Hf sulfate solutions suggests that the 12-member condensed core (hexamer edge-sharing with two pentamers) might be a stable cationic solution entity. However, this core, which contains no sulfate ions, is not indicated in the SAXS data of hafnium chloride only. This suggests this core cannot form without the sulfate ligands. The fact that Hf_{18} does not persist in solution, nor can it be redissolved even remotely intact, can also be rationalized by the capacity of hafnium to assume a variety of labile coordination geometries. Although sulfate coordinates very strongly to hafnium, it can also interconvert readily between monodentate, bidentate, and bridging. Disorder between sulfate and hydroxyl groups was observed in the crystal structure of the Zr_{18}, suggesting the anions undergo dynamic exchange in solution.[11]

Finally, ESI-MS data of hafnium oxychloride solutions and hafnium oxychloride−sulfate solutions, with and without peroxide, provided consistent evidence for the predominance of the Hf tetramer and Hf pentamer in solution, while the Hf hexamer is only a minor component. Figures 8−10 summarize these results. All data were collected in the positive mode, meaning the observed species carry a positive charge. A 200 mM solution of Hf oxychloride with 0.5 equiv of peroxide (Figure 8) initially has two m/z envelopes, both consistent with

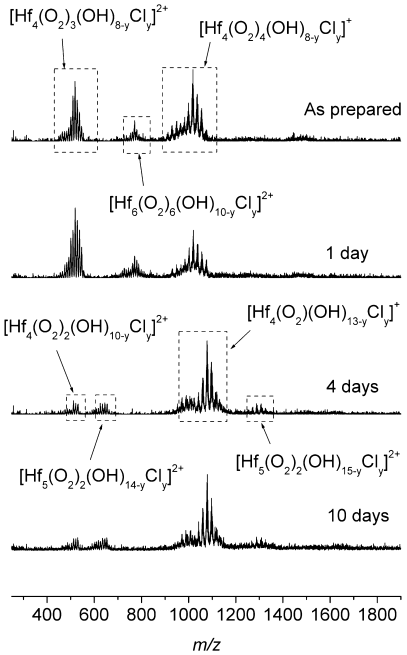

Figure 8. ESI-MS (positive mode) of a 200 mM $HfOCl_2$ solution with peroxide and $HfOCl_2/H_2O_2$ = 1:0.5. See Supporting Information, Figure SI5 for detailed peak assignments. Values for x and y range from 0 to 8.

Hf tetramer species. Both also have associated peroxide, one in a 4:4 and the other in a 4:3 Hf/peroxide ratio. There is also a smaller peak series that is identified as the Hf hexamer, also with a 1:1 Hf/peroxide ratio. With aging time, one tetramer envelope and the hexamer envelope evolve to pentameric Hf species. After 10 d, the solution is still dominated by tetramers, but with a significant amount of pentameric species. The peroxide/Hf ratio has also decreased, which confirms our prior observations and the well-known fact that peroxide decomposes with time, especially when catalyzed by a polarizing metal cation. The final peroxide/Hf ratio in the clusters after 10 d is

dx.doi.org/10.1021/ic500375v | Inorg. Chem. 2014, 53, 4234−4242

close to 1:2. Note that this is the same peroxide/Hf ratio of the initial solution, but we do not detect the significantly polymerized Hf, as discussed in more detail below.

The Hf sulfate solutions, with and without peroxide (Figures 9 and 10, respectively), clearly show the role of the peroxide in keeping the Hf sulfate clusters in solution. With peroxide, the clusters persist in solution for 4 d. Without peroxide, there is no evidence of cluster species after 1 d. Although the SAXS studies showed soluble species for up to one week, the analyses processes between SAXS and MS differ. ESI-MS requires injection of solution into a small opening and vaporization of the soluble species. Perhaps these process steps reject the larger species that evolve with solution aging. Nonetheless, the data clearly suggest peroxide solubilizes Hf sulfate clusters. Like the Hf oxychloride solutions, Hf tetramers and Hf pentamers clearly dominate Hf sulfate solutions, with and without peroxide. The peroxide/Hf ratio is lower in these solutions, likely because the sulfate displaces the peroxide ligands. In the detailed peak assignments (see Supporting Information, Figures SI6 and SI7 and Figures 9 and 10), the number of OH^- ligands and Cl^- ligands (x and y in Figures 8–10) varies considerably, while the ratio of Hf/sulfate and Hf/peroxide is fairly consistent within a series of related species. This suggests that the OH^- and Cl^- anions are loosely associated, while the sulfate and peroxide ligands are an integral part of the Hf clusters. These data are entirely consistent with the SAXS data that suggests small clusters like Hf tetramers and pentamers link through sulfate ligands to form the chain-like assemblies that grow with time. The aforementioned chains detected by SAXS are likely fragmented into their Hf cluster building blocks (tetramers, pentamers, and hexamers) by the ionization process.

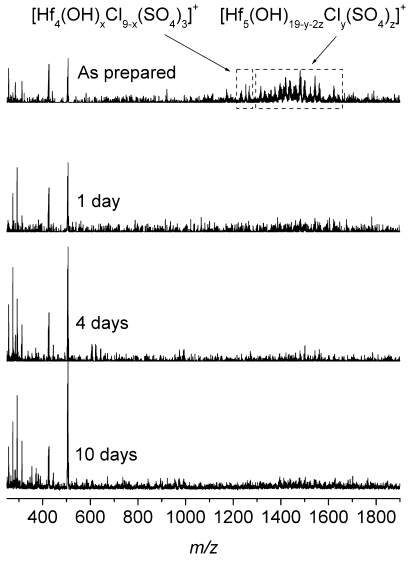

Figure 9. ESI-MS (positive mode) of a 200 mM $HfOCl_2$ solution with sulfate and no peroxide and $HfOCl_2/H_2SO_4$ = 1:0.7. See Supporting Information, Figure SI6 for detailed peak assignments. Values for x and y range from 3 to 14.

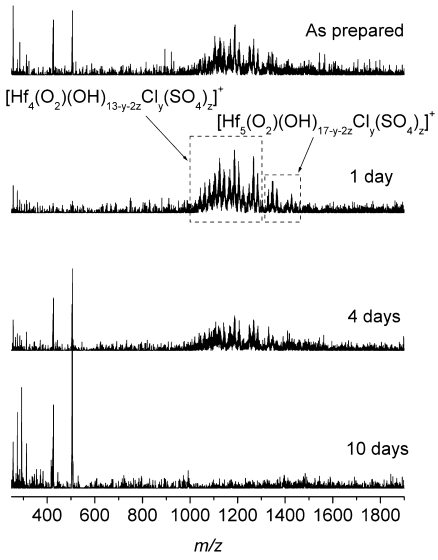

Figure 10. ESI-MS (positive mode) of a 200 mM $HfOCl_2$ solution with sulfate, peroxide, and $HfOCl_2/H_2SO_4/H_2O_2$ = 1:0.7:0.5. See Supporting Information, Figure SI7 for detailed peak assignments. Values for x and y range from 1 to 10.

CONCLUSIONS

The fundamental question we have explored with this study is simple: is self-assembly of the Hf_{18} polyoxometalate cluster an important intermediate step between Hf sulfate–peroxide precursor solutions and HfO_2 thin films. The frequency and ease of crystallization of Hf_{18} from the precursor solutions suggest that it is a relevant intermediate. However, our studies presented here show that Hf_{18} is never observed in solution, nor can it be redissolved intact: this is not entirely surprising in that Hf_{18} is a neutral species. What is surprising is that nothing bigger than a Hf hexamer is ever observed in solution, with the exception of evidence for the side-by-side octamer in less concentrated hafnium oxychloride solution and Hf sulfate solutions, after Hf_{18} has precipitated. Moreover, even the hexamer is far less abundant than the tetramer and pentamer, and the hexamer converts to tetramers and/or pentamers with time. With the addition of sulfate, the tetramers/pentamers/hexamers still persist but become linked into chains, presumably via sulfate bridging, which is also not consistent with the Hf_{18} structure. Since hexamers and pentamers are the core building blocks of Hf_{18}, they likely condense and precipitate as the sulfate-capped Hf_{18} very rapidly; the elusive intermediates, like the Hf_{12} core for instance, have not yet been captured by solution or solid-state studies. High lattice energy of solid Hf_{18} is likely the driving force of its frequent crystallization from precursor solutions, and thus the Hf_{18} cluster is not likely to be found in the amorphous gels that are deposited by spin coating of these solutions. To obtain our smooth and dense films, crystallization of the deposited gel cannot occur. This means that the gel is likely to be structurally similar to that which we ascertained from the solution studies presented here: small Hf tetramers, pentamers, and hexamers bridged by sulfates in a network. Future studies interpreting the structure of the Hf sulfate gel, as well as comparing the energetics of the thermodynamically stable Hf_{18} to the kinetically obtained gel intermediates, will be the next step in unraveling this complex chemical system.

EXPERIMENTAL SECTION

Solution Preparation. A hafnium stock solution was prepared from $HfOCl_2 \cdot 8H_2O$ (98+%, Alfa Aesar) and 18.2 MΩ purified water at approximately 1 M concentration. The exact concentration was determined gravimetrically by conversion of a known volume of solution to solid hafnium oxide. One molar H_2SO_4 (BDH Chemicals)

dx.doi.org/10.1021/ic500375v | Inorg. Chem. 2014, 53, 4234–4242

and 30 wt % H_2O_2 (Macron) were used as received. All hafnium sulfate solutions were prepared by mixing $HfOCl_2$ and H_2SO_4 solutions and diluting with 18.2 MΩ purified water. The sulfate to hafnium molar ratio was maintained at 0.7. We verified with single-crystal X-ray diffraction that the Hf_{18} crystallizes from solutions with this composition. For solutions that contain peroxide, the peroxide to hafnium molar ratio was maintained at 0.5. The molarity of each solution is given with respect to hafnium.

Small-Angle X-ray Scattering. Small-angle X-ray scattering data were collected on an Anton Paar SAXSess instrument utilizing Cu Kα radiation (1.54 Å) and line collimation. Solutions were measured in 1.5 mm glass capillaries. Pure water was used for the background, and scattering was typically measured for 30 min. SAXSQUANT software was used for data collection and treatment (normalization, primary beam removal, background subtraction, desmearing, and smoothing to remove extra noise created by the desmearing routine). Guinier analysis was performed in the linear region at low q ($q < R_g^{-1}$) and fit within IgorPro 6 (Wavemetrics software). All other analyses and fits to determine size, shape, and PDDF were carried out utilizing the IRENA macros within IgorPro. Modeling II macros were used for cylindrical fits and structure factor analysis. Size distributions were constrained to be highly monodisperse (full width at half-maximum $<10^{-4}$ Å). Structure factor analysis used the interferences model.[72] PDDF, probability ($p(r)$) as a function of radial distance from the edge of the particle ($r = 0$), were determined using the Moore method[84] in IRENA.[73] SolX software was used to simulate scattering data from crystal structures.[77,78]

Raman Spectroscopy. Raman spectra were collected on a Thermo Scientific DXR SmartRaman spectrometer with a 780 nm laser source. Spectra were deconvoluted into Gaussian peaks using the multipeak fit macros in IgorPro. Sloping baselines were removed from the spectra for clarity.

Electrospray Ionization Mass Spectrometry. ESI-MS was carried out using an Agilent G1956b 1100 series LC/MSD single-quadrupole mass spectrometer using a cone voltage of −20 V and at an injection rate of 0.1 mL/min with a syringe pump for direct source injection. The solutions of $HfOCl_2$ at 200 mM concentration with/without H_2O_2 and H_2SO_4 were separately prepared, and small aliquots of solutions were directly injected to the instrument for analysis with the interval of days. The data were collected at positive mode, and all the presented spectra are averaged signal acquired for 1 min. The peak assignments were made by using Isotopic Distribution Modeling function in Molecular Weight Calculator software (freeware: M. Monroe, Molecular Weight Calculator ver. 6.49). The peak assignments were carried out by combinations of Hf^{4+}, O_2^{2-}, Cl^-, or SO_4^{2-}. The regular spacing between peaks matched with mass difference by adding or subtracting O_2^{2-}, Cl^-, or SO_4^{2-}. The complex multiplicity of each peak arises from the combined isotopic patterns of the components, hafnium in particular.

■ ASSOCIATED CONTENT

Supporting Information

SAXS intensity data, PDDF data, and detailed peak assignments in ESI-MS spectra for hafnium sulfate solutions. This material is available free of charge via the Internet at http://pubs.acs.org.

■ AUTHOR INFORMATION

Corresponding Author

*E-mail: may.nyman@oregonstate.edu.

Notes

The authors declare no competing financial interest.

■ ACKNOWLEDGMENTS

This work was funded by the National Science Foundation, Grant CHE-1102637, via the Center for Sustainable Materials Chemistry.

■ REFERENCES

(1) Addadi, L.; Raz, S.; Weiner, S. *Adv. Mater.* **2003**, *15*, 959.
(2) Meldrum, F. C.; Cölfen, H. *Chem. Rev.* **2008**, *108*, 4332.
(3) Penn, R. L.; Banfield, J. F. *Am. Mineral.* **1998**, *83*, 1077.
(4) Penn, R. L.; Banfield, J. F. *Geochim. Cosmochim. Acta* **1999**, *63*, 1549.
(5) Navrotsky, A. *Proc. Natl. Acad. Sci. U.S.A.* **2004**, *101*, 12096.
(6) Niederberger, M.; Cölfen, H. *Phys. Chem. Chem. Phys.* **2006**, *8*, 3271.
(7) Anderson, J. T.; Munsee, C. L.; Hung, C. M.; Phung, T. M.; Herman, G. S.; Johnson, D. C.; Wager, J. F.; Keszler, D. A. *Adv. Funct. Mater.* **2007**, *17*, 2117.
(8) Meyers, S. T.; Anderson, J. T.; Hung, C. M.; Thompson, J.; Wager, J. F.; Keszler, D. A. *J. Am. Chem. Soc.* **2008**, *130*, 17603.
(9) Clearfield, A. *Rev. Pure Appl. Chem.* **1964**, *14*, 91.
(10) Macdermott, T. E. *Coord. Chem. Rev.* **1973**, *11*, 1.
(11) Squattrito, P. J.; Rudolf, P. R.; Clearfield, A. *Inorg. Chem.* **1987**, *26*, 4240.
(12) Ahmed, M. A. K.; Fjellvag, H.; Kjekshus, A. *Acta Chem. Scand.* **1999**, *53*, 24.
(13) Muha, G. M.; Vaughan, P. A. *J. Chem. Phys.* **1960**, *33*, 194.
(14) Aberg, M. *Acta Chem. Scand., Ser. A* **1977**, *31*, 171.
(15) Toth, L. M.; Lin, J. S.; Felker, L. K. *J. Phys. Chem.* **1991**, *95*, 3106.
(16) Singhal, A.; Toth, L. M.; Lin, J. S.; Affholter, K. *J. Am. Chem. Soc.* **1996**, *118*, 11529.
(17) Hu, Y.-J.; Knope, K. E.; Skanthakumar, S.; Kanatzidis, M. G.; Mitchell, J. F.; Soderholm, L. *J. Am. Chem. Soc.* **2013**, *135*, 14240.
(18) Pan, L.; Heddy, R.; Li, J.; Zheng, C.; Huang, X. Y.; Tang, X. Z.; Kilpatrick, L. *Inorg. Chem.* **2008**, *47*, 5537.
(19) Fitzgerald, M.; Pappas, I.; Zheng, C.; Xie, Z. L.; Huang, X. Y.; Tao, S.; Pan, L. *Dalton Trans.* **2009**, 6289.
(20) Starikova, Z. A.; Turevskaya, E. P.; Kozlova, N. I.; Turova, N. Y.; Berdyev, D. V.; Yanovsky, A. I. *Polyhedron* **1999**, *18*, 941.
(21) Kuznetsov, V. Y.; Dikareva, L. M.; Rogachev, D. L.; Poraikoshits, M. A. *J. Struct. Chem.* **1985**, *26*, 923.
(22) Kalaji, A.; Soderholm, L. *Chem. Commun.* **2014**, *50*, 997.
(23) Connick, R. E.; McVey, W. H. *J. Am. Chem. Soc.* **1949**, *71*, 3182.
(24) Ahrland, S.; Karipides, D.; Noren, B. *Acta Chem. Scand.* **1963**, *17*, 411.
(25) Thompson, R. C. *Inorg. Chem.* **1985**, *24*, 3542.
(26) Ichinose, H.; Terasaki, M.; Katsuki, H. *J. Ceram. Soc. Jpn.* **1996**, *104*, 715.
(27) Zhang, Y.; Wu, L. Z.; Zeng, Q. H.; Zhi, J. F. *J. Phys. Chem. C* **2008**, *112*, 16457.
(28) Jiang, K.; Anderson, J. T.; Hoshino, K.; Li, D.; Wager, J. F.; Keszler, D. A. *Chem. Mater.* **2011**, *23*, 945.
(29) Park, J. H.; Yoo, Y. B.; Lee, K. H.; Jang, W. S.; Oh, J. Y.; Chae, S. S.; Baik, H. K. *ACS Appl. Mater. Interfaces* **2013**, *5*, 410.
(30) Piquemal, J. Y.; Briot, E.; Bregeault, J. M. *Dalton Trans.* **2013**, *42*, 29.
(31) Agarwal, M.; De Guire, M. R.; Heuer, A. H. *J. Am. Ceram. Soc.* **1997**, *80*, 2967.
(32) Niesen, T. P.; De Guire, M. R.; Bill, J.; Aldinger, F.; Ruhle, M.; Fischer, A.; Jentoft, F. C.; Schlogl, R. *J. Mater. Res.* **1999**, *14*, 2464.
(33) Yadav, G. D.; Nair, J. J. *Microporous Mesoporous Mater.* **1999**, *33*, 1.
(34) Ciesla, U.; Froba, M.; Stucky, G.; Schuth, F. *Chem. Mater.* **1999**, *11*, 227.
(35) Yamabi, S.; Imai, H. *Chem. Mater.* **2002**, *14*, 609.
(36) Yan, M. C.; Chen, F.; Zhang, J. L.; Anpo, M. *J. Phys. Chem. B* **2005**, *109*, 8673.
(37) Hu, M. Z.; DeBaillie, A. C.; Wei, Y. Y.; Jellison, G. E. *Curr. Nanosci.* **2006**, *2*, 13.
(38) Stanciu, C.; Jones, M. E.; Fanwick, P. E.; Abu-Omar, M. M. *J. Am. Chem. Soc.* **2007**, *129*, 12400.
(39) Bassil, B. S.; Mal, S. S.; Dickman, M. H.; Kortz, U.; Oelrich, H.; Walder, L. *J. Am. Chem. Soc.* **2008**, *130*, 6696.

(40) Mal, S. S.; Nsouli, N. H.; Carraro, M.; Sartorel, A.; Scorrano, G.; Oelrich, H.; Walder, L.; Bonchio, M.; Kortz, U. *Inorg. Chem.* **2010**, *49*, 7.
(41) Carraro, M.; Nsouli, N.; Oelrich, H.; Sartorel, A.; Soraru, A.; Mal, S. S.; Scorrano, G.; Walder, L.; Kortz, U.; Bonchio, M. *Chem.—Eur. J.* **2011**, *17*, 8371.
(42) Colfen, H.; Schnablegger, H.; Fischer, A.; Jentoft, F. C.; Weinberg, G.; Schlogl, R. *Langmuir* **2002**, *18*, 3500.
(43) Chiavacci, L. A.; Santilli, C. V.; Pulcinelli, S. H.; Craievich, A. F. *J. Appl. Crystallogr.* **1997**, *30*, 750.
(44) Chiavacci, L. A.; Bourgaux, C.; Briois, V.; Pulcinelli, S. H.; Santilli, C. V. *J. Appl. Crystallogr.* **2000**, *33*, 592.
(45) Chiavacci, L. A.; Santilli, C. V.; Pulcinelli, S. H.; Bourgaux, C.; Briois, V. *Chem. Mater.* **2004**, *16*, 3995.
(46) Kanazhevskii, V. V.; Shmachkova, V. P.; Kotsarenko, N. S.; Kolomiichuk, V. N.; Kochubei, D. I. *J. Struct. Chem.* **2006**, *47*, 860.
(47) Chiavacci, L. A.; Pulcinelli, S. H.; Santilli, C. V.; Briois, V. *Chem. Mater.* **1998**, *10*, 986.
(48) Rosa, M. A. A.; Sanhueza, C. S. S.; Santilli, C. V.; Pulcinelli, S. H.; Briois, V. *J. Phys. Chem. B* **2008**, *112*, 9006.
(49) Kanazhevskii, V. V.; Novgorodov, B. N.; Shmachkova, V. P.; Kotsarenko, N. S.; Kriventsov, V. V.; Kochubey, D. I. *Mendeleev Commun.* **2001**, 211.
(50) Mark, W.; Hansson, M. *Acta Crystallogr., Sect. B: Struct. Sci.* **1975**, *31*, 1101.
(51) Dalgarno, S. J.; Atwood, J. L.; Raston, C. L. *Inorg. Chim. Acta* **2007**, *360*, 1344.
(52) Oleksak, R. P.; Ruther, R. E.; Luo, F.; Fairley, K. C.; Decker, S. R.; Stickle, W. F.; Johnson, D. W.; Garfunkel, E. L.; Herman, G. S.; Keszler, D. A. *ACS Appl. Mater. Interfaces* **2014**.
(53) Stowers, J.; Keszler, D. A. *Microelectron. Eng.* **2009**, *86*, 730.
(54) Telecky, A.; Xie, P.; Stowers, J.; Grenville, A.; Smith, B.; Keszler, D. A. *J. Vac. Sci. Technol., B* **2010**, *28*, C6S19.
(55) Stowers, J. K.; Telecky, A.; Kocsis, M.; Clark, B. L.; Keszler, D. A.; Grenville, A.; Anderson, C. N.; Naulleau, P. P. *Proc. SPIE 7969, Extreme Ultraviolet (EUV) Lithography II* **2011**, 796915.
(56) Dengel, A. C.; Griffith, W. P. *Polyhedron* **1989**, *8*, 1371.
(57) Tarafder, M. T. H.; Miah, M. A. L. *Inorg. Chem.* **1986**, *25*, 2265.
(58) Tarafder, M. T. H.; Bhattacharjee, P.; Sarkar, A. K. *Polyhedron* **1992**, *11*, 795.
(59) Chen, H.; Irish, D. E. *J. Phys. Chem.* **1971**, *75*, 2672.
(60) Myneni, S. C. B. *Rev. Mineral. Geochem.* **2000**, *40*, 113.
(61) Riemer, T.; Spielbauer, D.; Hunger, M.; Mekhemer, G. A. H.; Knozinger, H. *J. Chem. Soc., Chem. Commun.* **1994**, 1181.
(62) Zhang, Y. H.; Chan, C. K. *J. Phys. Chem. A* **2000**, *104*, 9191.
(63) Zhang, Y. H.; Chan, C. K. *J. Phys. Chem. A* **2002**, *106*, 285.
(64) Zhao, L. J.; Zhang, Y. H.; Wei, Z. F.; Cheng, H.; Li, X. H. *J. Phys. Chem. A* **2006**, *110*, 951.
(65) Guo, X.; Xiao, H. S.; Wang, F.; Zhang, Y. H. *J. Phys. Chem. A* **2010**, *114*, 6480.
(66) Szilagyi, I.; Konigsberger, E.; May, P. M. *Inorg. Chem.* **2009**, *48*, 2200.
(67) Bensitel, M.; Saur, O.; Lavalley, J. C.; Morrow, B. A. *Mater. Chem. Phys.* **1988**, *19*, 147.
(68) Spielbauer, D.; Mekhemer, G. A. H.; Bosch, E.; Knozinger, H. *Catal. Lett.* **1996**, *36*, 59.
(69) Li, C.; Stair, P. C. *Catal. Lett.* **1996**, *36*, 119.
(70) Ise, N. *Angew. Chem., Int. Ed. Engl.* **1986**, *25*, 323.
(71) Glatter, O.; Kratky, O. *Small Angle X-ray Scattering;* Academic Press, Inc.: London, 1982.
(72) Beaucage, G.; Ulibarri, T. A.; Black, E. P.; Schaefer, D. W. In *Hybrid Organic-Inorganic Composites;* American Chemical Society: Washington, DC, 1995; Vol. *585*, p 97.
(73) Ilavsky, J.; Jemian, P. R. *J. Appl. Crystallogr.* **2009**, *42*, 347.
(74) Glatter, O. *J. Appl. Crystallogr.* **1980**, *13*, 577.
(75) Pedersen, J. S. *Adv. Colloid Interface Sci.* **1997**, *70*, 171.
(76) Hou, Y.; Zakharov, L. N.; Nyman, M. *J. Am. Chem. Soc.* **2013**, *135*, 16651.
(77) Zhang, R. T.; Thiyagarajan, P.; Tiede, D. M. *J. Appl. Crystallogr.* **2000**, *33*, 565.
(78) Tiede, D. M.; Zhang, R. T.; Chen, L. X.; Yu, L. H.; Lindsey, J. S. *J. Am. Chem. Soc.* **2004**, *126*, 14054.
(79) Hansson, M. *Acta Chem. Scand.* **1969**, *23*, 3541.
(80) Hansson, M. *Acta Chem. Scand.* **1973**, *27*, 2455.
(81) Hansson, M. *Acta Chem. Scand.* **1973**, *27*, 2614.
(82) Elbrahimi, M.; Durand, J.; Cot, L. *Eur. J. Solid State Inorg. Chem.* **1988**, *25*, 185.
(83) Gascoigne, D.; Tarling, S. E.; Barnes, P.; Pygall, C. F.; Benard, P.; Louer, D. *J. Appl. Crystallogr.* **1994**, *27*, 399.
(84) Moore, P. B. *J. Appl. Crystallogr.* **1980**, *13*, 168.